



HAL
open science

Role of reserve carbohydrates in the growth dynamics of *Saccharomyces cerevisiae*

Vincent Guillou, Lucile Plourde-Owobi, Jean Luc Parrou, Gérard Goma, Jean
François

► **To cite this version:**

Vincent Guillou, Lucile Plourde-Owobi, Jean Luc Parrou, Gérard Goma, Jean François. Role of reserve carbohydrates in the growth dynamics of *Saccharomyces cerevisiae*. *FEMS Yeast Research*, 2004, 4 (8), pp.773-787. 10.1016/j.femsyr.2004.05.005 . hal-02559445v2

HAL Id: hal-02559445

<https://hal.insa-toulouse.fr/hal-02559445v2>

Submitted on 5 May 2020

HAL is a multi-disciplinary open access archive for the deposit and dissemination of scientific research documents, whether they are published or not. The documents may come from teaching and research institutions in France or abroad, or from public or private research centers.

L'archive ouverte pluridisciplinaire **HAL**, est destinée au dépôt et à la diffusion de documents scientifiques de niveau recherche, publiés ou non, émanant des établissements d'enseignement et de recherche français ou étrangers, des laboratoires publics ou privés.

Role of reserve carbohydrates in the growth dynamics of *Saccharomyces cerevisiae* [☆]

Vincent Guillou ¹, Lucile Plourde-Owobi ^{1,2}, Jean Luc Parrou, Gerard Goma, Jean François ^{*}

Centre de Bioingénierie Gilbert Durand, Laboratoire Biotechnologie et Bioprocédés, UMR-CNRS 5504 & UMR-INRA 792, 31077 Toulouse Cedex 04, France

Abstract

The purpose of this study was to explore the role of glycogen and trehalose in the ability of *Saccharomyces cerevisiae* to respond to a sudden rise of the carbon flux. To this end, aerobic glucose-limited continuous cultures were challenged with a sudden increase of the dilution rate from 0.05 to 0.15 h⁻¹. Under this condition, a rapid mobilization of glycogen and trehalose was observed which coincided with a transient burst of budding and a decrease of cell biomass. Experiments carried out with mutants defective in storage carbohydrates indicated a predominant role of glycogen in the adaptation to this perturbation. However, the real importance of trehalose in this response was veiled by the unexpected phenotypes harboured by the *tps1* mutant, chosen for its inability to synthesize trehalose. First, the biomass yield of this mutant was 25% lower than that of the isogenic wild-type strain at dilution rate of 0.05 h⁻¹, and this difference was annulled when cultures were run at a higher dilution rate of 0.15 h⁻¹. Second, the *tps1* mutant was more effective to sustain the dilution rate shift-up, apparently because it had a faster glycolytic rate and an apparent higher capacity to consume glucose with oxidative phosphorylation than the wild type. Consequently, a *tps1gcy1gcy2* mutant was able to adapt to the dilution rate shift-up after a long delay, likely because the detrimental effects from the absence of glycogen was compensated for by the *tps1* mutation. Third, a *glg1Δglg2Δ* strain, defective in glycogen synthesis because of the lack of the glycogen initiation protein, recovered glycogen accumulation upon further deletion of *TPS1*. This recovery, however, required glycogen synthase. Finally, we demonstrated that the rapid breakdown of reserve carbohydrates triggered by the shift-up is merely due to changes in the concentrations of hexose-6-phosphate and UDPglucose, which are the main metabolic effectors of the rate-limiting enzymes of glycogen and trehalose pathways.

Keywords: Trehalose; Glycogen; Continuous cultures; Yeast dynamics; Metabolic regulation

1. Introduction

The yeast *Saccharomyces cerevisiae* is endowed with a remarkable metabolic flexibility which enables it to cope

with large nutrient fluctuations in the environment. Typical metabolic key-points in this metabolic adaptation are glycogen and trehalose, which either accumulate or are mobilized according to environmental and stress conditions [1–3]. Glycogen and trehalose have important functions with respect to metabolic adaptation, including carbon and energy reserves and stress protection [4]. Convincing evidence that a major function of glycogen is to provide carbon and energy for maintenance of cellular activities was obtained with respiration-deficient cells which, contrary to wild-type cells, readily mobilize the accumulated glycogen immediately

[☆] Supplementary data associated with this article can be found, in the online version, at doi:10.1016/j.femsyr.2004.05.005.

^{*} Corresponding author. Present address: Département Génie Biochimique et Alimentaire, 135 Avenue de Rangueil, 31077 Toulouse Cedex, France. Tel.: +33-5-61-55-94-92; fax: +33-5-61-55-94-00.

E-mail address: fran_jm@insa-tlse.fr (J. François).

¹ Both authors have equally contributed to this work.

² Present address: Aventis Pasteur Biomérieux, Lyon, France.

at the onset of glucose depletion [3]. Conversely, a role of trehalose in stress protection has been recognized based on the observation that the capacity of yeast cells to withstand harmful conditions is correlated with a high intracellular content of trehalose [5,6]. Moreover, trehalose has two unique properties that make it a stress protectant, namely its capacity to protect membranes from desiccation, and its ability to exclude water from the protein surface and hence protect proteins from denaturation in dehydrated cells [7–9]. Moreover, trehalose metabolism plays a role in control of the glycolytic flux as indicated by the finding that growth on rapidly fermentable sugars is prevented in a *tps1* mutant which is deficient in the catalytic subunit of the trehalose-6-P synthase complex. The precise molecular mechanism has not yet been completely worked out although there are strong indications that this control occurs at the level of the hexose phosphorylation step [10,11].

Another potential function of glycogen and trehalose is in the progression of the cell division. An initial indication of this implication was obtained with continuous cultures of yeast at low dilution rates which exhibited spontaneous cell cycle-related oscillations. These oscillations were characterized by periodic changes of dissolved oxygen, ethanol production, biomass concentration, budding index and cellular content of storage carbohydrates [12–16]. More recently, Verrips and coworkers [17–19] have used partially synchronised carbon-limited continuous cultures of yeast and shown that below a certain sugar flux, imposed by reducing the dilution rate, the content of glycogen and trehalose increased proportionally to the length of the G1 phase of the cell cycle. The two glucose stores were subsequently mobilized before entrance of the cells into the S phase. On the basis of these data, it was proposed that the mobilisation of storage carbohydrates temporarily increased the sugar flux, thus enabling the cells to go through a next round of division [18]. Contrary to expectation, a mutant completely unable to synthesize both glycogen and trehalose was still able to divide at

low growth rate under carbon-limited conditions, although the passage to a next cell division was much slower than that of the wild type [18]. Moreover, these authors showed that the carbon flow that was saved on carbohydrate synthesis was fully oxidized, which indicated that the mutant cells had a higher ATP flux than the wild type. This higher energy dissipation was assumed to be the price to pay for enabling these mutant cells to divide under deteriorating growth conditions [18].

In the present work, we sought an alternative approach to investigate the role of glycogen and trehalose in cell division and growth. The strategy was to increase the carbon flux of glucose-limited continuous cultures of a wild-type strain, and mutants defective in glycogen and trehalose, by a dilution rate shift-up from 0.05 to 0.15 h⁻¹. This methodological approach brought several unexpected results, including a predominant role of glycogen in this metabolic perturbation and new traits associated with inactivation of the *TPS1* gene.

2. Materials and methods

2.1. Yeast strains and construction of mutants

The *Saccharomyces cerevisiae* strain CEN.PK113-7D [20], referred to as the ‘wild type’ (WT) in this study, and its *ura3-52* derivative CEN.PK113-5D were used as host strains for *TPS1*, *GLG1*, *GLG2*, *GSY1* and *GSY2* disruptions (Table 1). Two alleles of *TPS1* were used in this study. The *tps1Δ::kanMX4* allele is identical to the *tps1::loxP-kanMX-loxP* allele that has been described in [21]. It was obtained by PCR with d-TPS1 and f-TPS1 primers (Table 2). The *tps1Δ::URA3-hisG* allele was constructed from pALK752, a pBSK vector carrying *TPS1* ORF with promoter and terminator sequences [22], and pNKY51 which bears the *hisG-URA3-hisG* disruption cassette [23]. Deletion of the 1.15-kb *NcoI* fragment in pALK752 yielded pJF579 (*tps1Δ*). The *BamHI/BglII hisG-URA3-hisG* module from pNKY51

Table 1
Strain used in this study

Strain	Genotype	References
CENPK133-7D	Mat a	[20]
CEN.PK133-5D	Mat a <i>ura3-52</i>	[20]
JF1055	Mat a <i>tps1Δ::Kan^R</i>	This work
JF1468	Mat a <i>ura2-52 tps1Δ::URA3</i>	This work
JF971	Mat a <i>glg1Δ::Kan^R GLG2</i>	This work
JF955	Mat a <i>GLG1 glg2Δ::Kan^R</i>	This work
JF969	Mat a <i>glg1Δ::Kan^R glg2Δ::Kan^R</i>	This work
JF1446	Mat α <i>ura3-52 tps1Δ::URA3 glg1Δ::Kan^R glg2Δ::Kan^R</i>	This work
JF1486	Mat α <i>ura3-52 GSY1 gsy2Δ::URA3-hisG tps1Δ::hisG</i>	This work
JF1484	Mat α <i>ura3-52 gsy1Δ::URA3-hisG GSY2 tps1Δ::hisG</i>	This work
JF1494	Mat α <i>ura3-52 gsy1Δ::hisG gsy2Δ::URA3-hisG tps1Δ::hisG</i>	This work

Table 2
Primers used for gene disruption

Name	Sequence (5' > 3')	Short description
GLG1-300	GTTAGAGGAAGCAGGCAAAA	Primer used for <i>GLG1</i> cloning
GLG1 + 450	TTCTTCGAAACCCTAACCGA	Primer used for <i>GLG2</i> cloning
d-GLG2	ATGGCCAAGAAAGTTGCCATCTGTACATTGCTGTATTCACCAGCTGAAGCTTCGTACCGC	Primer used for <i>GLG2</i> disruption by the method of Wach et al. [25]
f-GLG2	TCAGGTATCAGGCTTTGGGAATGCTTTGGACGGTCTGCATAGGCCACTAGTGGATCTG	Primer used for <i>GLG2</i> disruption by the method of Wach et al. [25]
d-TPS1	ATGACTACGGATAACGCTAAGCGCAACTGACCTCGTCTTCAAGCTGAAGCTTCGTACCGC	Primer used for <i>TPS1</i> disruption by the method of Wach et al. [25]
f-TPS1	TCAGTTTTGTGGCAGAGGAGCTTGTGGAGCTGATGATGCATAGGCCACTAGTGGATCTG	Primer used for <i>TPS1</i> disruption by the method of Wach et al. [25]
JL37	ATGTCCCGTGACCTACAAAACCAATTTGTTATTCGAGACTGCGACTGAGGTCGAAAAGTGC- CACCTGACG	Primer used for <i>GSY2</i> disruption using then <i>hisG-URA3-hisG</i> cassette of Alami et al. [23]
JL38	TTAACTGTCATCAGCATATGGGCCATCGTCGTCATCGTGCAGGATCAAGCGCTCAT- GAGCCCG	Primer used for <i>GSY2</i> disruption using then <i>hisG-URA3-hisG</i> cassette of Alami et al. [23]

was inserted into the *Bgl*II site of pJF579 to yield to pJF805 (*tps1Δ::URA3-hisG*). The 5.2-kb *Xho*I/*Xba*I *tps1Δ::URA3-hisG* cassette from pJF805 was used to replace wild-type *TPS1* in CEN.PK113-5D by homologous recombination.

Disruption of *GLG1* by the *KanMX4* module was carried out as follows. The *GLG1* gene was amplified by PCR from genomic DNA using GLG1-300 and GLG1 + 450 primers (Table 2) and the PCR product was cloned into the pGEM-T (Promega) to yield pGEM-T-GLG1. The 632 pb *EcoRV/Hpa*I fragment from this construct, was replaced by the 1.5-kb *Sma*I/*Hpa*I *kanMX4* cassette from pFA6a-*kanMX4* [25] to yield pGEM-T-*glg1::kanMX4*. The 2.4-kb *BspE1/Nhe*I fragment from the latter plasmid was then used for genomic disruption of wild-type *GLG1* in CEN.PK113-7D. Disruption of *GLG2* was carried out by direct replacement of *GLG2* by transformation of CEN.PK113-7D according to [24], using the *loxP-KanMX4-loxP* module of pUG6 [25] and primers d-GLG2 and f-GLG2 (Table 2). These two primers have 40 nucleotide-5' extensions that are homologous to the region downstream of the start codon and upstream of the stop codon of *GLG2*, respectively. The *glg1Δglg2Δ* double mutant strain (JF1969) was isolated after tetrad dissection of a *glg1Δ/GLG1glg2Δ/GLG2* heterozygous diploid by the lack of glycogen accumulation under vapor iodine staining [3], and verified by PCR according to Wach et al. [25].

The *GSY1* disruption was carried out using pGSY1, which bears a 4.2-kb *Hind*III genomic fragment with *GSY1* (kind gift from P. Roach, Indianapolis University). The 2.3-kb *Bcl*I fragment of pGSY1 was replaced by the 3.85-kb *Bam*H1/*Bgl*II *hisG-URA3-hisG* cassette from pNKY51 to yield pJL45. Genomic replacement was performed by transformation of CEN.PK113-5D strain with the 5.3-kb *Spe*I/*Xba*I fragment from pJL45. For *GSY2* disruption, we used pRS314-*GSY2*, which carries a 3.4-kb *EcoRV* *GSY2* genomic DNA fragment in the *Sma*I restriction site of pRS314 (gift from P. Roach, Indianapolis University). A PCR amplification of the *hisG-URA3-hisG* cassette from pNKY51 was carried out with primers JL37 and JL38 (Table 2), which have 40 nucleotide-5' extensions homologous to the region immediately downstream of the start codon and upstream of the stop codon of *GSY2*, respectively. Co-transformation of this PCR product with pRS314-*GSY2* linearized at *Bst*B1 in *GSY2* allowed in vivo recombination and the recovery of pJL46 (pRS314-*gsy2Δ::URA3-hisG*). The *Sac*I/*Kpn*I fragment from pJL46 that contains *gsy2Δ::URA3-hisG* allele was used for the transformation of the CEN.PK113-5D strain. To remove the *URA3* marker, mutant strains were replica-plated onto 5-fluorouracil plates which led to the excision of the gene by homologous recombination between flanking *hisG* repeats. This method led to strains with

tps1Δ::hisG, *gsy1Δ::hisG* or *gsy2Δ::hisG* alleles. Genetic crosses, sporulation on 1% (w/v) K acetate agar plate followed by tetrad dissection led to mutant strains with multiple gene disruptions. Mutants were selected by lack of glycogen accumulation [3] for disruption of *GSY1* and *GSY2*, and lack of growth on SD-fructose plates (0.17% yeast nitrogen base without ammonium and amino acid, 0.5% ammonium sulphate, 2% agar and 2% fructose) for *tps1* mutation. Genes disruption was verified by Southern blotting or PCR.

2.2. Shake-flask cultivation

Stationary-phase cells cultured on YPD medium (2% glucose, 1% yeast extract, 2% bacto-peptone) were kept frozen in 25% glycerol at -80°C . The frozen cells were used to inoculate fresh YPD agar plates. A single colony was inoculated in 5 ml mineral medium prepared according to Verduyn et al. [26] which contained 23 g l^{-1} galactose as the carbon source. After 10 h of growth at 30°C , this culture was transferred to a 0.5-l shake flask containing 100 ml of the same medium for 12 h at 30°C .

2.3. Chemostat cultures

The shake-flask culture was used to inoculate a 2-l fermentor SETRIC 2M (Inceltech-SGI, Toulouse, France) containing 1.1 l of mineral medium prepared according to Verduyn et al. [30] and 23 g l^{-1} galactose. Aerobic chemostat cultivation was performed at 30°C , the medium supply was started when galactose was completely consumed. The influx of medium was provided by a peristaltic pump. The defined medium for carbon-limited chemostat cultivation contained per litre of demineralised water: glucose, 15 g; $(\text{NH}_4)_2\text{SO}_4$, 5 g; KH_2PO_4 , 3 g; $\text{MgSO}_4 \times 7\text{H}_2\text{O}$, 0.5 g; 1 ml trace element and 1 ml vitamin solution prepared according to Verduyn et al. [26]. The working volume of the cultures was kept constant at 1.1 l by means of an electric level floating sensor. A stirrer speed of 800 rpm and an air flow of 1.5 l min^{-1} kept the partial oxygen pressure always at minimally 50% of its saturation value as measured with an Ingold oxygen probe. The pH was controlled at 5.0 by automatic addition of 2-M NaOH.

2.4. Shift-up experiments in chemostat

The aerobic glucose – limited chemostat cultivation was set up at a dilution rate of 0.05 h^{-1} . Although instabilities of the culture due to spontaneous oscillatory behaviour occasionally happened, cultures used for steady-state analysis or shift-up experiments did not exhibit detectable metabolic oscillations. Yeast cultures were assumed to be at steady-state at the dilution rate of 0.05 h^{-1} when after five reactor-volumes changes, the cell biomass, rates of CO_2 production and O_2 consumption

differed by less than 5% and no oscillation of the CO_2 production rate occurred during this period. Shift-up experiments from 0.05 to 0.15 h^{-1} dilution rate were achieved on these steady-state cultures by setting a three times increase in the feeding rate. Elemental balances during the transients were checked on cumulated quantities of metabolites as described by Poilpre et al. [28].

2.5. Determination of cell number and budding index

Samples of cultures were mildly sonicated and counted under an optical microscope. The percentage of budded cells (budding index) was estimated over at least 200 cells, and this counting was repeated at least three times on independent samples and by two independent investigators.

2.6. Determination of macroscopic parameters

Dry mass was determined gravimetrically from filtered culture samples (10–30 ml) on preweighed nitrocellulose filters (pore size $0.45\text{ }\mu\text{m}$, Sartorius). The filters were washed with demineralised water and dried in oven set at 80°C for 24 h. Alternatively, the dry mass could be obtained on-line by measurement of the luminance using a spectrometer ACS ICS as described previously [28]. Elemental composition of biomass was obtained from samples harvested from the chemostat at different times during the fermentation. Samples were lyophilised and C, H, O, N content were measured with a Perkin–Elmer elemental analyser. Based on the elemental analysis, a molecular formula $\text{CH}_{1.851}\text{O}_{0.61}\text{N}_{0.167}$ for CENPK113-7D was obtained at both dilution rates (0.05 and 0.15 h^{-1}), which corresponds to a molecular mass of 25.97 gC mol^{-1} and a degree of reduction γ of 4.25. This value is very close to the published data of Lange and Heijnen [29] who used the same strain. This value was used for estimation of the carbon balances. The molar fractions of O_2 and CO_2 for inlet and exhaust gases were determined on-line by a mass spectrometer (PRIMA 600S, VG Gas, Manchester, UK) with a relative accuracy of 0.1%. The fermentor was flushed with dry air by a mass flow controller (New Brunswick Scientific, France). CO_2 production rate r_{CO_2} and O_2 consumption rate r_{O_2} were calculated according to [27].

2.7. Enzymatic assays

Preparation of extracts for enzymatic assays was performed according to François et al. [30]. Glycogen synthase (active form) was measured with 0.25 mM UDP-[U- ^{14}C]Glucose as the substrate. Glycogen phosphorylase was measured in the reverse reaction by incorporation of [U- ^{14}C] glucose into glycogen using 5 mM [U- ^{14}C] glucose-1-P. Trealose-6-P synthase was

assayed by the formation of UDP formed as described by Vandercammen et al. [31], except that the temperature of the enzymatic assay was set at 45 °C to avoid interference with glycogen synthase which is totally inactive at this temperature. Neutral trehalase was assayed according to Neves and François [32].

2.8. Determination of glycogen, trehalose, and extracellular metabolites

Samples (2 ml) were quickly harvested by a syringe from the fermentor, centrifuged 2 min at 4000g in eppendorf tubes. The pellet was used for enzymatic determination of glycogen and trehalose according to [33]. Glucose, glycerol, ethanol and acetate were determined in the cell-free supernatant with commercial biochemical kits or by high-performance liquid chromatography. In the latter case, the supernatant was filtered through 0.22- μm -pore-size nylon filters prior to loading on a HPX-87H Aminex ion exclusion column. The column was eluted at 48 °C with 5 mM H_2SO_4 at a flow rate of 0.5 ml min^{-1} and the concentration of the compounds was determined using a Waters model 410 refractive index detector. Extracellular organic acids were determined by high performance ionic chromatography (HPIC) using a Dionex Bio-LC500 apparatus as described previously [34].

3. Results

3.1. Physiological characteristics of wild-type and mutant strains defective in reserve carbohydrates during steady-state growth at 0.05 and 0.15 h^{-1}

The glucose-limited chemostat culture was initiated from batch cultures of yeast grown to the late-exponential phase on galactose. The continuous culture of the wild-type strain at a growth rate of 0.05 h^{-1} was exclusively oxidative with a biomass yield (Y_{XS}) of

0.47 g g^{-1} , a respiratory quotient (RQ) close to 1.0 (Table 3a), and a residual glucose in the fermentor below 10 mg l^{-1} . Under this condition, yeast cells accumulated large amounts of trehalose and glycogen that reached, respectively, 4.90% and 11.80% of the dry mass. At a higher dilution rate of 0.15 h^{-1} , the metabolism remained oxidative while the amount of glycogen had decreased to 3.80% and trehalose was no longer detectable (Table 3b). These effects of dilution rates on the reserve carbohydrates content were consistent with previous reports [12,16–18].

Mutants defective in trehalose synthesis were generated by disruption of *TPS1* encoding the catalytic subunit of the trehalose-6-P synthase complex [35]. As reported in Tables 3a and 3b, glucose-limited continuous cultures of *tps1 Δ were achieved at low dilution rate of 0.05 and 0.15 h^{-1} , likely because the carbon flux under these growth conditions was much lower than that caused by excess glucose in batch cultures, which leads to growth inhibition [11]. However, at the low growth rate of 0.05 h^{-1} , the biomass yield (Y_{XS}) of *tps1 Δ was 25% lower than that of the wild type, and this lower biomass yield was accompanied by a 25% increase in the specific rate of CO_2 production and O_2 consumption. Moreover, the deletion of *TPS1* enhanced glycogen deposition by about 30%. Therefore, the reduction in biomass of a *tps1* mutant cannot be attributed to a decrease in storage carbohydrates since in wild-type and mutant cells a similar amount of carbon had been diverted into glucose stores. These differences in biomass and respiration rate between *tps1* and wild-type cells were no longer observed when the continuous culture was carried out at a dilution rate of 0.15 h^{-1} (Table 3b).**

Mutants unable to accumulate glycogen were generated by deletion of *GLG1* and *GLG2* which encode the redundant glycogenin proteins that are required for glycogen initiation [36]. As shown in Tables 3a and 3b, the macro-kinetic parameters of the *glg1* Δ *glg2* Δ strain (i.e. Y_{XS} , q_{glucose} and RQ) were similar to those of the isogenic wild-type strain at the two dilution rates of

Table 3a

Physiological parameters of wild-type and mutant strains defective in glycogen and trehalose accumulation during steady-state growth at a dilution rate of 0.05 h^{-1}

Genotype	$X \text{ g l}^{-1}$	$Y_{\text{XS}} X$ (g glucose) $^{-1}$	q mCmol $\text{g}^{-1} \text{ h}^{-1}$			RQ ($q_{\text{CO}_2}/q_{\text{O}_2}$)	Glycogen (% dry mass)	Trehalose (% dry mass)
			q_{Glucose}	q_{CO_2}	q_{O_2}			
Wild type	6.95	0.47	3.60	2.2	2.02	1.08	11.8	4.9
<i>tps1</i> Δ	5.60	0.38	4.4	2.9	2.9	1.0	15.2	<0.1
<i>glg1</i> Δ <i>glg2</i> Δ	7.35	0.49	3.40	1.85	1.85	1.0	<1.0	4.5
<i>tps1</i> Δ <i>glg1</i> Δ <i>glg2</i> Δ	5.5	0.37	4.6	2.7	2.7	1.0	5.6	<0.1
<i>tps1</i> Δ <i>ggsy1</i> Δ <i>ggsy2</i> Δ	5.20	0.35	4.8	2.60	2.50	1.04	bd	bd

bd: below detection.

X is the biomass concentration at steady-state in g l^{-1} ; Y_{XS} is the yield of biomass (in g dry mass) per gram of glucose in the reservoir.

q_{CO_2} and q_{O_2} are the specific rates of CO_2 production and O_2 consumption, respectively. They are calculated from gas balances and are expressed in $\text{mCmol g}^{-1} \text{ h}^{-1}$ or $\text{mmol g}^{-1} \text{ h}^{-1}$, where $\text{mCmol} = \text{mmol atom C}$ of a compound.

Table 3b

Physiological parameters of wild-type and mutant strains defective in glycogen and trehalose accumulation during steady-state growth at a dilution rate of 0.15 h⁻¹

Genotype	X g l ⁻¹	$Y_{XS} X$ (g glucose) ⁻¹	q_{Glucose}	q_{CO_2}	q_{O_2}	RQ ($q_{\text{CO}_2}/q_{\text{O}_2}$)	Glycogen (% dry mass)	Trehalose (% dry mass)
			mCmol g ⁻¹ h ⁻¹					
Wild type	6.95	0.46	10.8	6.2	6.0	1.03	3.8	bd
<i>tps1</i> Δ	6.9	0.47	10.7	6.5	6.4	1.01	6.0	bd
<i>glg1</i> Δ <i>glg2</i> Δ	6.75	0.45	11.1	5.7	5.9	0.97	bd	0.25
<i>tps1</i> Δ <i>glg1</i> Δ <i>glg2</i> Δ	6.3	0.42	11.9	6.4	6.4	1.0	2.0	bd
<i>tps1</i> Δ <i>gsy1</i> Δ <i>gsy2</i> Δ	6.6	0.44	11.3	5.1	4.8	1.06	bd	bd

bd: below detection.

See legend of Table 3a for definition of X , Y_{XS} , RQ and mCmol.

0.05 and 0.15 h⁻¹. In addition, the inability to synthesize glycogen did not alter trehalose accumulation, which contrasted with the effect of *TPS1* deletion to enhance glycogen deposition. Surprisingly, the disruption of *TPS1* in a *glg1*Δ*glg2*Δ mutant resulted in a partial recovery of glycogen accumulation (Table 3a) and in a drop of the biomass yield to a value similar to that of the *tps1* mutant at the low dilution rate of 0.05 h⁻¹. Further deletion of *GSY1* and *GSY2* encoding the two glycogen synthases [37] in the *tps1*Δ alone (Table 3a) or in the *tps1*Δ*glg1*Δ*glg2*Δ strain (data not shown) completely abolished the synthesis of glycogen. From these data, it can be concluded that the glycogenin-independent synthesis of glycogen in a *tps1* mutant required the elongation activity born by the glycogen synthase enzyme. However, the biomass yield of the *tps1*Δ*gsy1*Δ*gsy2*Δ strain at the steady-state growth of 0.05 h⁻¹ was the same as in *tps1* and *tps1*Δ*glg1*Δ*glg2* mutants, suggesting that the reduction in biomass at low growth rate was merely due to the loss of *TPS1* function rather than a consequence of the lack of storage carbohydrates.

3.2. Increase of budding is correlated with the mobilization of storage carbohydrates in response to the shift-up in the dilution rate

As indicated in Fig. 1, the reserve carbohydrates (glycogen + trehalose) were rapidly mobilized in response to a sudden increase of the dilution rate from 0.05 to 0.15 h⁻¹. In the wild-type CENPK strain, 2 h after the shift-up, the glucose stores dropped from 15% to 4% and then remained at this low level during steady-state cultivation at $D = 0.15$ h⁻¹. At this new dilution rate, the residual storage carbohydrate was glycogen, since trehalose was no longer detected (see Table 3b). The mobilization of glycogen and trehalose was accompanied by a transient increase in the budding index and by a decrease in cell biomass, both events peaking at their maximum *ca.* 1.5 h after the shift-up. At the dilution rate of 0.15 h⁻¹, the biomass recovered its initial value of about 7 g l⁻¹ after 20 h (>3 reactor-volume changes) and the budding index was stabilized at two times its initial value.

Similar experiments were carried out with mutants defective in the synthesis of either glycogen, trehalose or both in order to verify, and eventually to quantify, how far the transient rise of buds is linked to the breakdown of reserve carbohydrates. It can be seen in Fig. 1 that the lower was the content of reserve carbohydrates, the lower was the rise of the budding index after the shift-up. In particular, the *tps1*Δ*gsy1*Δ*gsy2*Δ mutant, which totally lacks storage carbohydrates, did not show any transient increase of buds within 1 h after the shift-up. To evaluate the correlation between increase of budding and mobilisation of reserve carbohydrates, we plotted the Δ budding index, which is the difference between the maximal budding and initial budding before the shift-up, versus the amount of reserve carbohydrates mobilized during the same interval of time. As illustrated in Fig. 2, a fairly good correlation between these two parameters with a coefficient of 0.95 was obtained. This is consistent with the suggestion of Sillje et al. [17] that the mobilisation of carbohydrates may provide a transient surplus of ATP required for progression through the cell cycle.

3.3. A wash-out effect accounts for the loss of biomass in a mutant defective in glycogen, while *tps1*Δ adapts faster than the wild type to the shift-up

As indicated in Fig. 1, the dry mass of the wild-type cells decreased by about 12% in 1.5 h after the shift-up to 0.15 h⁻¹. This loss of biomass was accompanied by an equivalent decrease of the storage carbohydrates in the cells, suggesting that the mobilisation of glycogen and trehalose can account for this loss of biomass. However, this correlation was not found in mutants defective in the synthesis of reserve carbohydrates. Notably, the decrease of biomass in a *tps1*Δ*gsy1*Δ*gsy2* mutant was almost comparable to that of the wild type, despite the fact that this mutant was totally devoid of glycogen and trehalose. Also, the loss of biomass of a *glg1*Δ*glg2*Δ strain was higher than in the isogenic wild type, even though the glycogen-defective mutant mobilized less storage carbohydrates. Conversely, the *tps1*Δ almost did

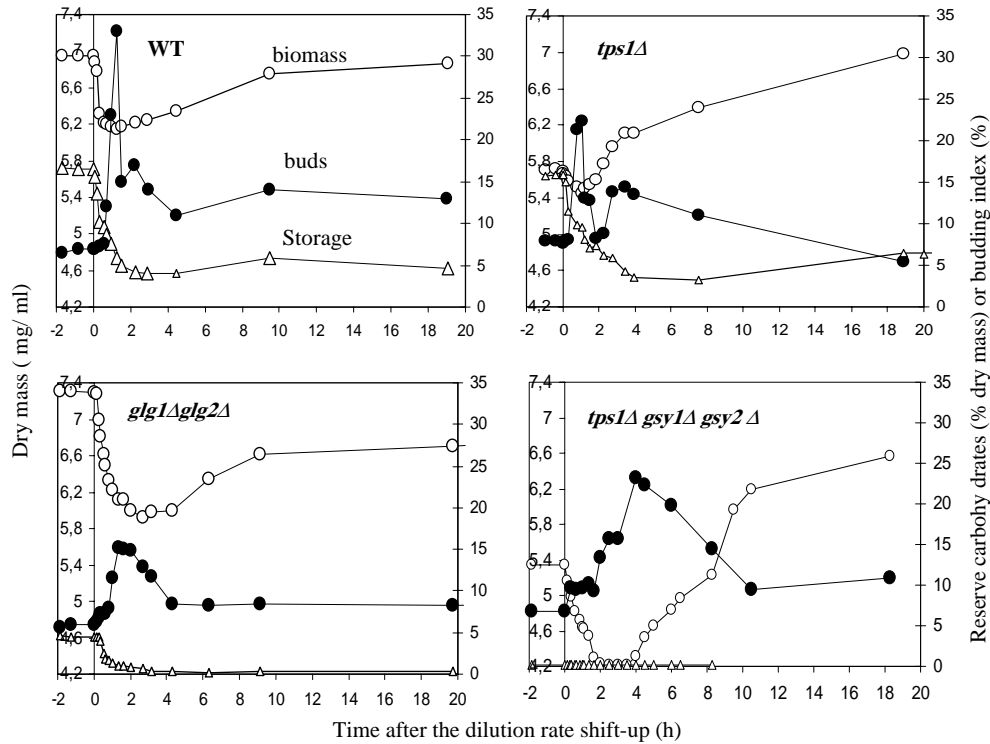


Fig. 1. Effect of the dilution rate shift-up on cell biomass, storage carbohydrates and budding index in continuous cultures of wild type and mutants defective in trehalose and glycogen. Cells were aerobically grown in a glucose-limited chemostat at a dilution rate of 0.05 h⁻¹. After reaching a steady-state (i.e. after more than five reactor-volume changes and no apparent oscillations), the culture was subjected to a sudden increase in dilution rate to 0.15 h⁻¹ by increasing the feeding rate in the fermentor. Samples were taken to measure biomass (○), glycogen and trehalose (△) and budding index (●) as described in Section 2.

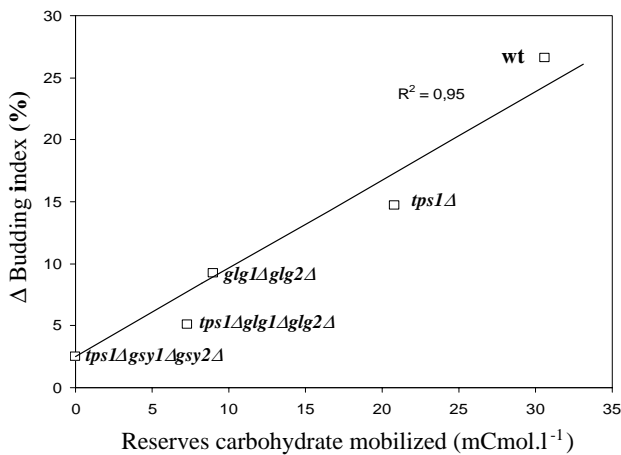


Fig. 2. Correlation between amount of reserve carbohydrates mobilized and percentage of budded cells in response to the shift-up in dilution rate from 0.05 to 0.15 h⁻¹. The data are taken from Fig. 1. The Δ buds (in %) is the difference between maximal budding before the shift-up. The amount of reserve carbohydrates mobilized corresponded to the difference between initial levels of glycogen + trehalose (expressed in mCmol l⁻¹) measured before the shift-up and those at the maximum of the budding index.

not lose biomass upon the shift-up, while it mobilized as much reserve carbohydrates as the wild-type strain (Fig. 1).

One possibility for this decrease in cell biomass is that part of the cell population has been washed out from the fermentor. This wash-out could arise from the fact that cell growth cannot withstand the rapid shift-up of the dilution rate. To quantify the importance of the wash-out, the effective decrease of biomass ($-\Delta X_{\text{eff}}$) and the amount of reserve carbohydrates that was mobilized ($-\Delta X_{\text{res}}$) were calculated during the same interval of time after the shift-up, and expressed in terms of mCmol l⁻¹ (Table 4). Accordingly, the difference, termed $-\Delta X_{\text{residual}}$, between these two parameters corresponded to the change of the cell biomass independent of the mobilisation of storage carbohydrates. Hence, an extreme situation would be that $-\Delta X_{\text{residual}}$ equalled $-\Delta X_{\text{maxth}}$, the maximal theoretical loss of biomass if complete growth inhibition had occurred upon the dilution rate shift-up at 0.15 h⁻¹. Table 4 recapitulates the values of these parameters measured for both wild-type and mutant strains. As already shown in Fig. 1, and confirmed in Table 4, the effective loss of biomass in the wild type ($-\Delta X_{\text{eff}}$) after the shift-up was equivalent to the amount of storage carbohydrates mobilized ($-\Delta X_{\text{res}}$), indicative of no wash-out after the shift-up. This was quantitatively confirmed by the calculation of the average μ , which is the difference between the actual dilution rate of 0.15 h⁻¹ and the effective wash-out of

Table 4

Carbon balance between the loss of biomass and reserve carbohydrates mobilized in wild-type and mutant strains at the peak of the budding index and/or at the minimal biomass concentration in response to the dilution shift-up at 0.15 h⁻¹ during Δt^*

Genotype	Δt^* (h)	ΔGly^1 (mCmol l ⁻¹)	ΔTre^2 (mCmol l ⁻¹)	ΔRes % DW	% Storages mobilized	$-\Delta X_{\text{eff}}^3$ (mCmol l ⁻¹)	$-\Delta X_{\text{res}}^4$ (mCmol l ⁻¹)	$-\Delta X_{\text{residual}}^5$ (mCmol l ⁻¹)	$-\Delta X_{\text{maxth}}^6$ (mCmol l ⁻¹)	Effective wash-out ⁷ (h ⁻¹)	Average μ^8 (h ⁻¹)
WT	1.5	20.9	9.73	11.54	70	30.0	32.4	-2.3	45.0	No	0.157
<i>tps1</i> Δ	1.05	19.9	0.00	9.09	57	10.0	20.7	-10.7	27.0	No	0.203
<i>ggl</i> Δ <i>gglg2</i> Δ	1.33	0.00	8.80	3.29	79	45.8	9.7	36.2	48.8	0.108	0.042
<i>ggl</i> Δ <i>gglg2</i> Δ <i>tps1</i> Δ	1.08	7.1	0.00	3.35	60	11.9	7.3	4.6	40.4	0.016	0.134
<i>ggy1</i> Δ <i>ggy2</i> Δ <i>tps1</i> Δ	2	0.00	0.00	0.00	0	34.3	0.0	34.3	52.2	0.093	0.057

* Δt^* is the time between t_0 (start of the dilution shift) and t_1 which corresponds to the peak of the budding index and/or at the minimal biomass concentration.

Equations used for calculation:

1 ΔGly (mCmol l⁻¹) = $(\text{Gly}_{t_0} \cdot X_{t_0} - \text{Gly}_{t_1} \cdot X_{t_1}) / (100 \times 180 / 162 \times 1000 / 30)$; with Gly:glycogen in% dry mass and X : biomass in g l⁻¹.

2 ΔTre (mCmol l⁻¹) = $(\text{Tre}_{t_0} \cdot X_{t_0} - \text{Tre}_{t_1} \cdot X_{t_1}) / (100 \times 360 / 342 \times 1000 / 30)$; with Tre: trehalose in% dry mass and X : biomass in g l⁻¹.

3 $-\Delta X_{\text{eff}}$ (mCmol l⁻¹) = $(X_{t_0} - X_{t_1}) / 25.97 \times 1000$; with X : biomass in g l⁻¹. This value corresponds to the effective decrease of biomass.

4 $-\Delta X_{\text{res}}$ (mCmol l⁻¹) = $X_{t_0} (\text{Res}_{t_0} / 100 - X_{t_1} (\text{Res}_{t_1} / 100 \times 1 / 25.97 \times 1000))$; with X : biomass in g l⁻¹ and Res = glycogen + trehalose in% dry mass. This value corresponds to the contribution of reserve carbohydrate mobilization.

5 $-\Delta X_{\text{residual}}$ (mCmol l⁻¹) = $\Delta X - \Delta X_{\text{res}}$. This value corresponds to the effective decrease/increase of the residual biomass independently of reserve carbohydrate mobilization.

6 $-\Delta X_{\text{maxth}}$ (mCmol l⁻¹) = $X_{\text{residual}-t_0} (1 - e^{-D \Delta t}) / 25.97 \times 1000$. This value corresponds to the theoretical variation of biomass during complete wash-out.

7 Effective wash-out (h⁻¹) = $-\ln(1 - \Delta X_{\text{residual}}^5 / 25.97 / 1000) / X_{\text{residual}-t_0} / \Delta t$. This value corresponds to the effective wash-out at the level of residual biomass.

8 Average $\mu = 0.15$ - Effective wash-out.

biomass (expressed in rate of residual biomass loss). The calculated value of 0.157 h⁻¹ was thus very close to the dilution rate, demonstrating that the wild-type cells immediately set the growth rate to the actual dilution rate.

With respect to the glycogen-defective mutant, we found that $-\Delta X_{\text{residual}}$ corresponded to 72% of the maximal loss of biomass from the fermentor ($-\Delta X_{\text{maxth}}$). Also, the loss of biomass in the triple *tps1ggy1ggy2* null mutant was due to the wash-out of the cells since this mutant was totally defective in glycogen and trehalose ($-\Delta X_{\text{res}} = 0$). An effective wash-out of 0.10 h⁻¹ of these two mutant strains was calculated, which gave rise to an average μ of 0.05 h⁻¹, i.e. close to the initial dilution rate before the shift-up (Table 4). This clearly indicated that these mutant cells were unable to immediately set the growth rate to the new dilution rate. Taken together, these results indicated an important role of glycogen in the capacity of yeast cells to respond to a sudden increase of the carbon flux in the range of low growth rates. This conclusion was substantiated in part by data with the *tps1ΔgglΔgglg2Δ* strain since this mutant, which has partially recovered glycogen accumulation, upon the shift had an average growth rate of 0.134 h⁻¹, close to the actual dilution rate of 0.15 h⁻¹ (Table 4).

In contrast to glycogen-defective strains, the effective loss of dry mass ($-\Delta X_{\text{eff}}$) of the *tps1*Δ was much lower than the amount of storage carbohydrates mobilized, resulting in a high negative value for $-\Delta X_{\text{residual}}$ (Table 4). This value indicated a rapid gain of cell biomass, which could be explained by the fact that the average growth rate of the *tps1*Δ was set at 0.203 h⁻¹ during the first hour after the shift-up. This effective growth rate, which was 35% higher than the actual dilution rate, showed that the *tps1*Δ mutant was more effective than the isogenic wild-type strain to withstand an increase of the carbon flux and to convert the glucose surplus into biomass in response to the shift-up.

3.4. Defects in carbohydrate storage cause a redistribution of the carbon flux between respiratory and oxido-reductive metabolism in response to the shift-up

In response to the shift-up, yeast cells are challenged with a sudden increase in the glucose flux. This carbon flux is the sum of the rate of exogenous glucose consumption and the rate of storage carbohydrates degradation (noted q_{HC} in Table 5). The increase of the flux triggered a transient metabolic shift from purely oxidative to oxido-reductive as indicated by a transient increase of the RQ (Fig. 3). This transient increase of RQ was lower in mutants defective in trehalose or glycogen, and it was completely absent in a mutant deficient in the two storage carbohydrates. The transition was also accompanied by a transient fivefold rise of the

Table 5

Contribution of reserve carbohydrates mobilization to the increase of the global carbon flux and repartition of the carbon flow into respiration and by-products formation, in response to the shift-up from 0.05 to 0.15 h⁻¹ during Δt ¹

Genotype	Δt (h)	X_{mean}^1 (g l ⁻¹)	ΔS^2 mCmol l ⁻¹	ΔRes^3	$\Delta \text{Res}/\Delta C$ (%)	r_{HC}^4 (mCmol l ⁻¹ h ⁻¹)	$\Delta C \rightarrow P^4$ mCmol l ⁻¹	q_{HC}^6 mCmol g ⁻¹ h ⁻¹	q_{OX}^6	q_p^6
WT	1.50	6.3	112.5	30.60	27	95.4	43.3	15.2	10.6	4.5
<i>tps1</i> Δ	1.05	5.5	78.8	19.9	25	94	25.6	16.9	12.5	4.4
<i>glg1</i> Δ <i>glg2</i> Δ	1.33	6.6	99.8	8.8	8.8	81.6	16.2	12.4	10.6	1.8
<i>tps1</i> Δ <i>glg1</i> Δ <i>glg2</i> Δ	1.08	5.3	81	7.1	8.8	81.6	22.9	15.4	11.4	4
<i>tps1</i> Δ <i>gsy1</i> Δ <i>gsy2</i> Δ	2.00	4.7	150	0.0	0	75.0	8.2	16	15.1	0.9

¹ Δt is the time between t_0 (start of the dilution shift) and t_1 which corresponds either to the peak of the budding index and/or at the minimal biomass concentration (X_{min}).

² $X_{\text{mean}} = \int_{t_0}^{t_1} X dt$.

³ ΔS and ΔRes are, respectively, the amount of glucose consumed and reserve carbohydrates mobilized during the Δt .

⁴ $r_{\text{HC}} = (\Delta S + \Delta \text{Res})/\Delta t$ is the global rate of carbon consumption during Δt .

⁵ $\Delta C \rightarrow P$ is the amount of carbon ($\Delta S + \Delta \text{Res}$) converted into by-products (ethanol, acetate and the glycerol) during Δt . The cumulated amount of the fermentation by-products was calculated according to [32].

⁶ q_{HC} ($= r_{\text{HC}}/X_{\text{mean}}$), q_{OX} ($= r_{\text{O}_2}/X_{\text{mean}}$) and q_p ($= q_{\text{HC}} - q_{\text{OX}}$) are the specific rates of total carbohydrate consumption, carbon oxidation, and carbon conversion to fermentation by-products during Δt .

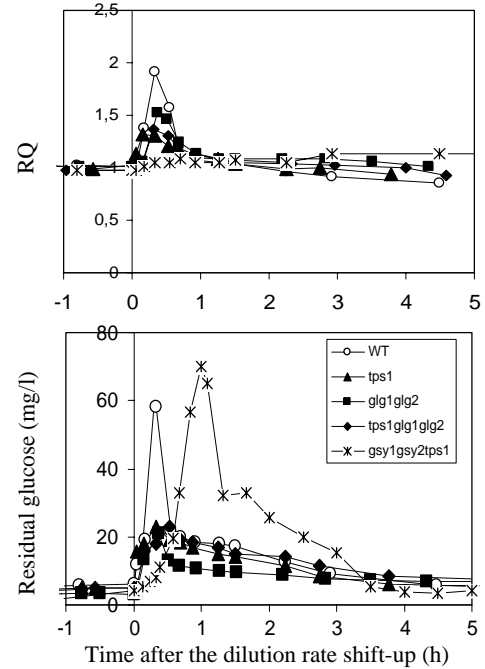


Fig. 3. Changes in the respiratory quotient and rates of mobilization of storage carbohydrates in response to the shift-up of the dilution rate. The data to calculate the rate of reserve carbohydrate are taken from Fig. 1. RQ is the respiratory coefficient which is the ratio $q_{\text{CO}_2}/q_{\text{O}_2}$. Symbols are: WT (○); *tps1* Δ (▲); *glg1* Δ *glg2* Δ (■); *tps1* Δ *glg1* Δ *glg2* Δ (◆) and *tps1* Δ *gsy1* Δ *gsy2* Δ (*).

extracellular glucose, suggesting a limitation at the hexose transport level or elsewhere in the metabolic pathway. This transient increase in the external glucose was lower in *tps1* and *glg1glg2* mutants, while it was higher than in wild type but strongly delayed in the *tps1gsy1gsy2* mutant. Another indication of this metabolic shift was given by the formation of by-products (ethanol, glycerol and acetate) which accumulated transiently in the culture medium after the dilution rate shift-up (Fig. 4). For the wild-type cells, the cumulated amount of the by-products (noted P) over a 1.5-h period after the shift-up represented 43 mCmol of the total carbon assimilated (ΔC). This amount was twofold higher than the amount of storage carbohydrate mobilized ($-\Delta \text{Res}$), indicating that a great part of the by-products formed upon the shift-up did not arise from the degradation of endogenous carbohydrate stores. This conclusion could be extended to *glg1glg2* and *tps1gsy1gsy2* mutants, but apparently not to the *tps1* Δ for which the cumulated formation of by-products was close to the amount of reserve carbohydrates mobilized.

Taking into account these metabolic changes, it was interesting to estimate how much carbon was distributed between fermentation and respiration in response to the dilution rate shift-up, and how this distribution was affected in mutants lacking carbohydrate reserves. Since the biomass production was different for each mutant strain, the carbon distribution was estimated by the

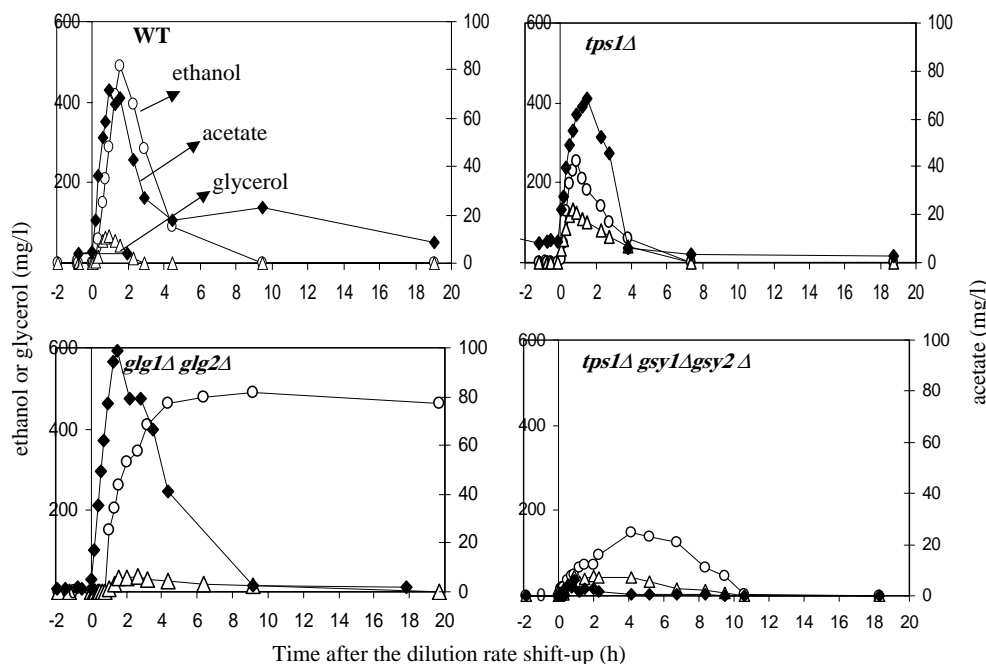


Fig. 4. Effect of the dilution rate shift-up on ethanol, glycerol and acetate production in wild-type and mutant strains defective in glycogen and trehalose synthesis. Growth conditions are those described in Fig. 1. Samples were taken to measure ethanol (○), glycerol (△) and acetate (◆) as described in Section 2.

specific rates of total sugar consumption (q_{HC}), oxidized carbon (q_{OX}) and carbon converted into by-products (q_P). As reported in Table 5, the q_{HC} and q_{OX} in $tps1\Delta$ were higher than in wild-type cells ($q_{HC} = 16.9$ versus 15.2 $\text{mCmol g}^{-1} \text{h}^{-1}$). This confirmed that the $tps1\Delta$ mutant had a greater ability to convert carbon into biomass after the shift-up, because of an apparent higher oxidative flux. This result could also explain why the transient rise of exogenous glucose and of the respiratory quotient were lower than that of the wild type (Fig. 3). Similarly, in $glg1\Delta glg2\Delta$ and in $tps1\Delta glg1\Delta glg2\Delta$, the contribution of respiration to the carbon consumption after the shift-up was also higher, consistent with a lower increase of the RQ than in wild-type cells (Fig. 3). This shift of carbon distribution towards respiration was even more pronounced in the $tps1\Delta gsy1\Delta gsy2\Delta$ mutant, where q_{OX} was the highest among the different mutants studied (Table 5). From these data, one could argue that respiration is more efficient in yeast cells lacking storage carbohydrates. However, in the triple mutant, this increase in respiration was only relative, because it was accompanied by a potent growth inhibition that lasted for 2 h after the shift-up. This can account for the delayed increase of glucose in the fermentor (Fig. 3).

3.5. Kinetic patterns of fermentation products in response to the shift-up

Fig. 4 shows the kinetic patterns of formation and reassimilation of fermentation by-products in wild-type

and mutant strains defective in the synthesis of trehalose, glycogen or in both reserve carbohydrates during 20 h after the shift-up from 0.5 to 0.15 h^{-1} . In the wild type, ethanol, glycerol and acetate accumulated with similar kinetics at a proportion of about 1:0.1:0.12 in the medium. The accumulation of the by-products was apparently faster in the $tps1\Delta$ strain, and more interestingly, this mutant produced two times more glycerol and two times less ethanol than the wild type. Similar traits, i.e. higher and faster glycerol production than in the wild types, were also seen in the $tps1\Delta glg1\Delta glg2\Delta$ mutant (data not shown). In contrast, ethanol and glycerol production were delayed in the $glg1\Delta glg2\Delta$ strain defective in glycogen synthesis, as compared with those in wild type and $tps1\Delta$. The $glg1\Delta glg2\Delta$ mutant was apparently unable to re-assimilate ethanol, but rather maintained a low steady state of ethanol production during a longer period of growth at $D = 0.15$ h^{-1} , to compensate for the dilution effect resulting from the chemostat cultivation. Finally, a weak production of ethanol and glycerol was also observed in the $tps1\Delta gsy1\Delta gsy2\Delta$ mutant. Since this mutant was totally defective in glycogen and trehalose, these by-products could only arise from the glucose surplus caused by the increase of the dilution rate.

3.6. Metabolic changes induced by the shift-up in wild type and mutants defective in storage carbohydrates

The remarkable metabolic perturbation triggered by the dilution rate shift-up prompted us to investigate

some pertinent intracellular metabolites in order to substantiate this perturbation at the level of the glycolytic metabolic pathway. To this end, we measured intracellular pools of glucose-6-P, fructose-1,6-P₂ and trehalose-6-P as main intermediates which could unravel some metabolic disorders occurring in response to the shift-up. Contrary to expectation, an increase of the

glucose influx caused a threefold decrease of glucose-6-P and trehalose-6-P (Fig. 5). This decrease in hexose-6-P was accompanied by a fourfold rise of fructose-1,6-P₂ which peaked 30 min after the shift-up, indicating a strong activation of the upper part of the glycolysis. Fructose-1,6-P₂ decreased to initial levels after 2 h, to increased subsequently and reached a constant value of

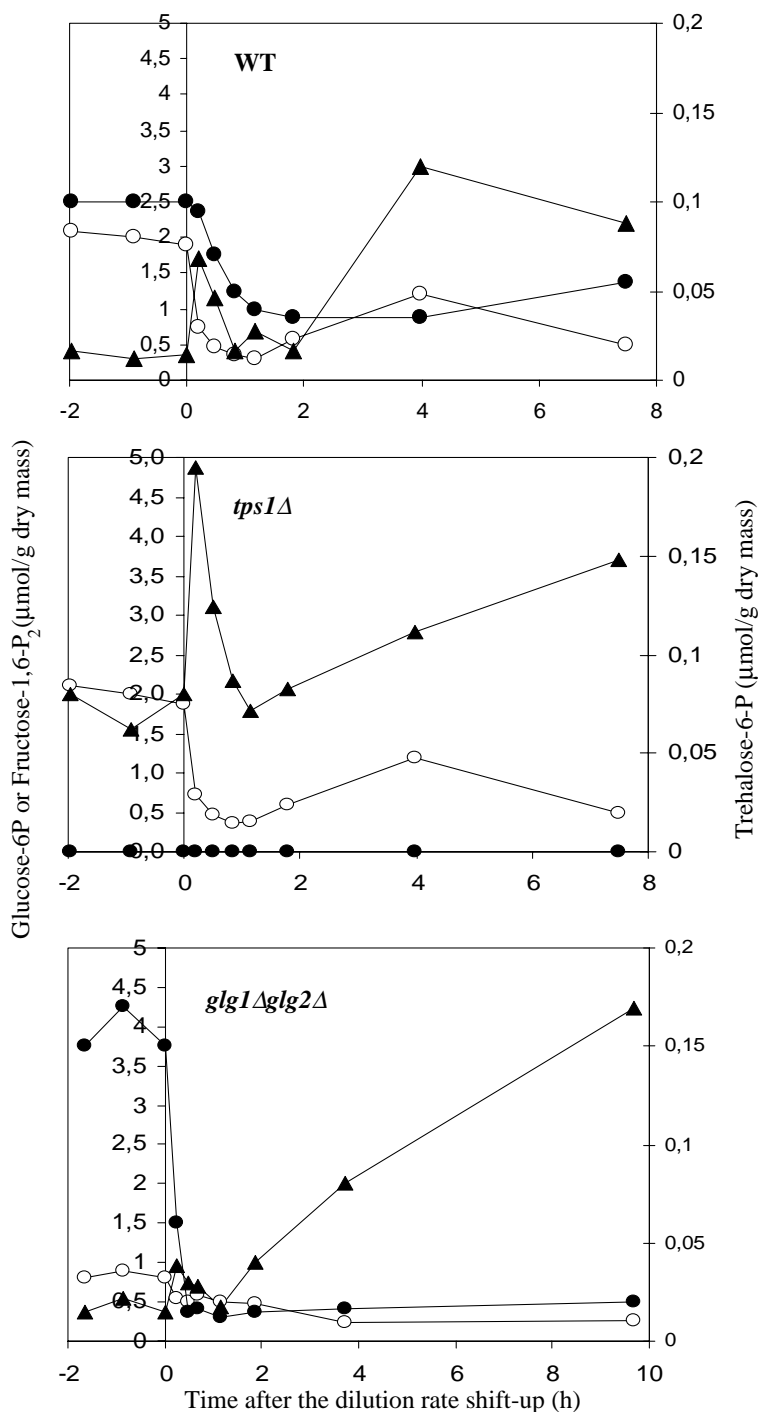


Fig. 5. Effect of the dilution rate shift-up on glucose-6-P, fructose-1,6-P₂ and trehalose-6-P levels in wild-type and mutant strains defective in glycogen and trehalose synthesis. Growth conditions are those described in Fig. 1. Samples were taken to measure glucose-6-P (○), fructose 1,6-P₂ (▲) and trehalose-6-P (●) as described in Section 2.

about 2.5 $\mu\text{mol g}^{-1}$ dry mass as the yeast returned to steady-state growth at the dilution rate of 0.15 h^{-1} . The *tps1* mutant, which as expected did not contain trehalose-6-P, also showed a rapid drop of glucose-6-P and an increase of fructose-1,6-P₂, similar to what was seen in the wild type, with the difference that the initial level of fructose-1,6-P₂ before the shift-up was fourfold higher in the *tps1* Δ . On the other hand, levels of glucose-6-P and fructose-1,6-P₂ in the *glg1glg2* mutant were lower than in the wild-type strain and were barely affected after the shift-up, whereas trehalose-6-P dropped very quickly, like in the wild type (Fig. 5). This result is indicative of a weak activation of glycolysis, and fits with the delay in the production of fermentation by-products observed in this mutant in response to the shift-up (Fig. 4).

3.7. Mobilization of storage carbohydrates induced by the shift-up is merely dependent on changes in metabolic effectors

The rapid mobilization of trehalose and glycogen in response to the dilution rate shift-up suggested that the activity of the key enzymes in glycogen and trehalose metabolism may be modified either by allosteric control or by covalent modification (for a review, see [4]). Thus, glycogen synthase (GS) and phosphorylase (GP), trehalose-6-P synthase (TPS) and trehalase (NTH) were measured before and 20 min after the shift-up. Contrary to expectation, the activity of these enzymes did not change significantly in response to the increase of carbon flux brought about by the shift-up (Table 6). Therefore, the rapid mobilization of storage carbohydrates did not appear to result from changes in enzyme activities by covalent modification, but was probably due to changes in metabolic effectors. In agreement with this suggestion, we reported in Fig. 5 that levels of glucose-6-P, a potent stimulator of glycogen synthase and inhibitor of glycogen phosphorylase, decreased immediately after the shift-up by about fourfold (from 2 to 0.5 $\mu\text{mol/g}$ dry mass, see Fig. 5), as well as UDP-glucose which decreased by about threefold (from 0.4 to

0.15 $\mu\text{mol/g}$ dry mass) (data not shown). As a consequence, a decrease of these two metabolites might suffice to impair glycogen and trehalose synthesis and to favour glycogen and trehalose breakdown.

4. Discussion

To investigate the relationship between carbon flux, cell growth and storage carbohydrates, we used mutants specifically defective in either one or both storage carbohydrates and employed the chemostat methodology to challenge yeast cells by an increase of the carbon flux. These experiments were carried out at low dilution rates since it is under these conditions that cells accumulate large amounts of glycogen and trehalose and that mobilisation of these storage carbohydrates is accompanied by bud emergence and stimulation of glycolysis [17,18,20]. Accordingly, we showed that the percentage of budded cells measured within a short period after the shift-up in the dilution rate from 0.05 to 0.15 h^{-1} correlated fairly well with the amount of reserve carbohydrates mobilized during this period. This result is consistent with the notion that mobilization of storage carbohydrates participates in the progression of the cell cycle by providing a surplus of ATP required at the bud emergence [17,18]. Moreover, it is well-established that within this range of dilution rate, aerobic glucose-limited continuous cultures display spontaneous oscillations that are supposed to arise from the breakdown of trehalose and glycogen [38,39]. Consistent with this idea, we found that a mutant totally defective in glycogen and trehalose (*tps1gsgsy2*) did not show any oscillatory behaviour during long-term cultivation at a low dilution rate of 0.05 h^{-1} (unpublished data).

Our experimental approach also brought new insight into the role of glycogen and trehalose in the ability of yeast cells to respond to a sudden increase of the carbon influx. An expected effect of this perturbation was that yeast cells unable to immediately adapt to the new dilution rate can be washed out from the fermentor. In this work, we provided evidence that glycogen plays an im-

Table 6
Enzymatic activities of the glycogen and trehalose pathways measured before and 20 min after the dilution rate shift-up

Genotype	Before the shift-up ($D = 0.05 \text{ h}^{-1}$)				After the shift-up at $D = 0.15 \text{ h}^{-1}$			
	Enzymatic activity (nmol/min \times mg protein)				Enzymatic activity (nmol/min \times mg protein)			
	GS (active form)	GP	TPS	NTH	GS (active form)	GP	TPS	NTH
Wild type	2.3	1.5	3.8	17	2.0	3.0	3.6	16
<i>tps1</i> Δ	2.5	13.0	0.0	18	2.0	18	0.0	11
<i>glg1</i> Δ <i>glg2</i> Δ	1.5	3.6	2.5	18	1.8	110	2.0	14.6
<i>tps1</i> Δ <i>glg1</i> Δ <i>glg2</i> Δ	1.0	9.4	0.0	12	1.0	14	0.0	15.7
<i>tps1</i> Δ <i>gsgsy1</i> Δ <i>gsgsy2</i> Δ	0.0	ND	0.0	ND	0.0	ND	0.0	ND

Active form = activity measured in the presence of 0.25 mM UDPglucose in the absence of glucose-6-P.

Abbreviations: GS, glycogen synthase; GP, glycogen phosphorylase; TPS, trehalose 6-P synthase; NTH, neutral trehalase.

ND = not determined. Values reported are the mean of two independent enzymatic measurements made on the same culture.

portant role to avoid this detrimental situation and hence that the mobilisation of this storage carbohydrate was critical to quickly adapt to an increase of the glucose influx under conditions of low growth rate. On the contrary, the loss of the *TPSI* function enhanced the aptitude of the yeast to respond to this carbon flux-up. We think that this finding is consistent with the role of *TPSI* to exert a negative control at the gate of the glycolysis [10,11], because under our experimental conditions, the increase in the glucose flux by the dilution rate shift-up is still far below the glycolytic flux of cells cultivated in a medium with excess glucose. Thus, rather than to be detrimental at low growth rates, the inactivation of *TPSI* provided some benefit to the cells to respond to a moderate increase of the glucose influx. This benefit was also associated with an apparent increased capacity to convert the glucose surplus into biomass by increasing the carbon flow into respiration. This positive effect on cell growth of disabling the *TPSI* function was further illustrated in a *glg1glg2* mutant whose loss of biomass due to the wash-out was largely reduced upon deletion of *TPSI*. Taken together, these results are consistent with the role of *TPSI* in controlling the glycolytic flux and also suggest a role in the control of the respiratory capacity of the cells. How this control might occur remains to be investigated. However, the fact that more glycerol than ethanol is formed in the *tps1* mutant following the shift-up should give some indication about this mechanism. Indeed, a higher flux in the glycerol pathway, which regenerates NAD^+ and P_i , is a means to reduce the metabolic flux through the lower part of glycolysis and thus possibly to avoid an overflow of the respiration at the level of the pyruvate node [40].

Another relevant result of this study was that the biomass yield (Y_{XS}) of strains harbouring a deletion of *TPSI* was about 25% lower than that of the wild-type strain when cultured at the low dilution rate of 0.05 h^{-1} . Since this effect was accompanied by an equivalent increase in the rate of CO_2 production and O_2 consumption, this pointed out that part of the sugar that had been spared for biomass production had been completely oxidized. This might provide the cells with more ATP to that was likely used for maintenance purposes. Alternatively, the respiratory chain could be less effective in this mutant at low growth rate, so that more carbon must be consumed to produce the same amount of ATP. In agreement with the latter suggestion, a recent genome-wide analysis of a *tps1* mutant revealed down-regulation of genes involved in respiration together with lower contents of cytochromes (Parrou, J.L., Teste, M.A., Rigoulet, M., and François, J., in preparation). Using a *tps1gcy1gcy2* mutant that is unable to synthesize trehalose and glycogen, Sillje et al. [18] also reported that more carbon was oxidized at low growth rates than in the isogenic wild type. They suggested that this increased oxidation and thus higher ATP production

stemmed from storage carbohydrates not being produced in this mutant. Our results contradict this conclusion because we found that any mutant defective in *TPSI* exhibited a higher rate of CO_2 production and O_2 consumption at low growth rate, independent of their content in storage carbohydrates. Therefore, the increasing energy expenditure with decreasing dilution rate is more likely a consequence of the absence of a functional *TPSI* gene rather than the lack of storage carbohydrates in the cells. Such a defect has never been identified before because previous work on *tps1* mutants was carried out in batch cultures in the presence of excess sugar, for which the glucose metabolism is typically oxido-reductive.

A third and also unexpected result of this study was to uncover a direct metabolic interaction between glycogen and trehalose. Indeed, we found for the first time that the synthesis of glycogen in yeast can be restored in a glycogenin-defective strain, when *TPSI* was further deleted in this mutant. Since glycogen synthase is unable to initiate glycogen directly from UDPglucose [41], but nevertheless was required for this glycogenin-independent synthesis, the possibility that another cryptic, yet uncharacterized initiating protein is responsible for this synthesis cannot be excluded. Alternatively, one can suggest that initiation of glycogen sets in on spurious short chains of oligosaccharides [41], which somehow would have been produced as a consequence of the inactivation of *TPSI*. Work is underway to identify the mechanism of glycogen synthesis induced by loss of *TPSI* in a *glg1glg2* mutant.

This study also showed that the mobilization of storage carbohydrates in response to an increase of the carbon flux is likely due to a decrease in the metabolic effectors, hexose-6-P and UDP-glucose, of the glycogen and trehalose metabolizing enzymes [42–45], and not to a change in the phosphorylated form of the key enzymes in these metabolisms. Our data are therefore at variance with those of Müller et al. [16] who have reported that spontaneous oscillations in a glucose-limited continuous culture at a dilution rate of 0.1 h^{-1} were associated with a concomitant peak of cAMP and with a transient activation of trehalase. At first glance, a decrease in hexose-6-P in response to a sudden up-shift in the dilution rate was not expected, taking into account that the glucose influx increased after the shift-up. However, the bulk increase of the glucose flux was only threefold, which is largely below the increase in the carbon flux caused by a glucose pulse to a steady-state continuous culture. In the latter situation, the large amount of added glucose probably overloaded the glycolytic capacity of the cells, while under our conditions, the glycolytic pathway was far from being saturated by this low increase of the glucose flow, and only a transient accumulation of metabolites occurred at key limiting steps of this metabolic pathway.

Acknowledgements

This work was supported in part by the 'Projet Intégré Génie des Procédés Biologiques' (PIRGP-BIO) of the CNRS. L.P.O. was supported by a doctoral grant from the French Ministry of Education and Research. We thank our colleagues for continuing support and critical reading of the manuscript.

References

- [1] Lillie, S.H. and Pringle, J.R. (1980) Reserve carbohydrate metabolism in *Saccharomyces cerevisiae*: responses to nutrient limitation. *J. Bacteriol.* 143, 1384–1394.
- [2] Parrou, J.L., Enjalbert, B., Plourde, L., Bauche, A., Gonzalez, B. and François, J. (1999) Dynamic responses of reserve carbohydrate metabolism under carbon and nitrogen limitations in *Saccharomyces cerevisiae*. *Yeast* 15, 191–203.
- [3] Enjalbert, B., Parrou, J.L., Vincent, O. and François, J. (2000) Mitochondrial respiratory mutants of *Saccharomyces cerevisiae* accumulate glycogen, and readily mobilize it in a glucose-depleted medium. *Microbiology* 146, 2685–2694.
- [4] François, J. and Parrou, J.L. (2001) Reserve carbohydrates in the yeast *Saccharomyces cerevisiae*. *FEMS Microbiol. Rev.* 25, 125–145.
- [5] Wiemken, A. (1990) Trehalose in yeast, stress protectant rather than reserve carbohydrate. *Antonie van Leeuwenhoek* 58, 209–217.
- [6] Attfeld, P.V. (1997) Stress tolerance: the key to effective strains of industrial baker's yeast. *Nature Biotechnol.* 15, 1351–1357.
- [7] Crowe, J.H., Hoekstra, F.A. and Crowe, L.M. (1992) Anhydrobiosis. *Annu. Rev. Physiol.* 54, 579–599.
- [8] Singer, M.A. and Lindquist, S. (1998) Thermotolerance in *Saccharomyces cerevisiae*: the Yin and Yang of trehalose. *Trends Biotechnol.* 16, 460–468.
- [9] Simola, M., Hanninen, A.L., Stranius, S.M. and Makarow, M. (2000) Trehalose is required for conformational repair of heat denaturated proteins in the yeast endoplasmic reticulum but not for maintenance of membrane traffic function after severe heat stress. *Mol. Microbiol.* 37, 42–53.
- [10] Teusink, B., Walsh, M.C., van Dam, K. and Westerhoff, H.V. (1998) The danger of metabolic pathways with turbo design. *Trends Biochem.* 23, 162–169.
- [11] Gancedo, C. and Flores, C.L. (2004) The importance of a functional trehalose biosynthetic pathway for the life of yeasts and fungi. *FEMS Yeast Res.* 4, 351–369.
- [12] Kuenzi, M.T. and Fiechter, A. (1972) Regulation of carbohydrate composition of *Saccharomyces cerevisiae* under growth limitation. *Arch. Microbiol.* 84, 254–265.
- [13] Porro, D., Martegani, E., Ranzi, B.M. and Alberghina, L. (1988) Oscillations in continuous cultures of budding yeast: a segregated parameter analysis. *Biotechnol. Bioeng.* 32, 411–417.
- [14] Martegani, E., Porro, D., Ranzi, B.M. and Alberghina, L. (1990) Involvement of a cell size control mechanism in the induction and maintenance of oscillations in continuous cultures of budding yeast. *Biotechnol. Bioeng.* 36, 453–459.
- [15] Duboc, P., Marison, I. and von Stockar, U. (1996) Physiology of *Saccharomyces cerevisiae* during cell cycle oscillations. *J. Biotechnol.* 51, 57–72.
- [16] Müller, D., Exler, S., Aguilera-Vazquez, L., Guerrero-Martin, E. and Reuss, M. (2003) Cyclic AMP mediates the cell cycle dynamics of energy metabolism in *Saccharomyces cerevisiae*. *Yeast* 20, 351–367.
- [17] Sillje, H.H.W., ter Schure, E.G., Rommens, A.J., Huls, P.G., Woldringh, C.L., Verkleij, A.J., Boonstra, J. and Verrips, C.T. (1997) Effects of different carbon fluxes on G1 phase duration, cyclin expression, and reserve carbohydrate metabolism in *Saccharomyces cerevisiae*. *J. Bacteriol.* 179, 6560–6565.
- [18] Sillje, H.H.W., Paalman, J.W.G., ter Schure, E.G., Olsthoorn, S.Q.B., Verkleij, A.J., Boonstra, J. and Verrips, C.T. (1999) Function of trehalose and glycogen in cell cycle progression and cell viability in *Saccharomyces cerevisiae*. *J. Bacteriol.* 181, 396–400.
- [19] Paalman, J.W.G., Verwaal, R., Slofstra, S.H., Verkleij, A.J., Boonstra, J. and Verrips, C.T. (2003) Trehalose and glycogen accumulation is related to the duration of the G1 phase of *Saccharomyces cerevisiae*. *FEMS Yeast Res.* 3, 261–268.
- [20] van Dijken, J.P., Bauer, J., Brambilla, L., Duboc, P., François, J., Gancedo, C., Giuseppin, M.L., Heijnen, J.J., Hoare, M., Lange, H.C., Madden, E.A., Niederberger, P., Nielsen, J., Parrou, J.L., Petit, T., Porro, D., Reuss, M., van Riel, N., Rizzi, M., Steensma, H.Y., Verrips, C.T., Vindelov, J. and Pronk, J.T. (2000) An interlaboratory comparison of physiological and genetic properties of four *Saccharomyces cerevisiae* strains. *Enzyme Microb. Technol.* 26, 706–714.
- [21] Plourde-Owobi, L., Durner, S., Parrou, J.L., Wiczorke, R., Goma, G. and François, J. (1999) *AGT1*, encoding an alpha-glucoside transporter involved in uptake and intracellular accumulation of trehalose in *Saccharomyces cerevisiae*. *J. Bacteriol.* 181, 3830–3832.
- [22] Vuorio, O.E., Kalkkinen, N. and Londesborough, J. (1993) Cloning of two related genes encoding the 56-kDa and 123-kDa subunits of trehalose synthase from the yeast *Saccharomyces cerevisiae*. *Eur. J. Biochem.* 216, 849–861.
- [23] Alani, E., Cao, L. and Kleckner, N. (1987) A method for gene disruption that allows repeated *URA3* selection in the construction of multiply disrupted yeast strains. *Genetics* 116, 541–545.
- [24] Güldener, U., Heck, S., Fiedler, T., Beinhauer, J. and Hegemann, J.H. (1996) A new efficient gene disruption cassette for repeated use in budding yeast. *Nucl. Acid Res.* 13, 2519–2524.
- [25] Wach, A., Brachat, A., Pöhlmann, R. and Philippsen, P. (1994) New heterologous modules for classical or PCR-based gene disruptions in *Saccharomyces cerevisiae*. *Yeast* 10, 1793–1808.
- [26] Verduyn, C., Postma, E., Scheffers, W.A. and Van Dijken, J.P. (1992) Effect of benzoic acid on metabolic fluxes in yeast: a continuous-culture study on the regulation of respiration and alcoholic fermentation. *Yeast* 8, 501–517.
- [27] Duboc, P. and von Stockar, U. (1995) Energetic investigation of *Saccharomyces cerevisiae* during transitions. Part I: Mass balances. *Thermochim. Acta* 251, 119–130.
- [28] Poilpre, E., Tronquit, D., Goma, G. and Guillou, V. (2002) On-line estimation of biomass concentration during transient growth of yeast chemostat culture using light reflectance. *Biotech. Lett.* 24, 2075–2081.
- [29] Lange, H.C. and Heijnen, J.J. (2000) Statistical reconciliation of the elemental and molecular biomass composition of *Saccharomyces cerevisiae*. *Biotechnol. Bioeng.* 75, 334–344.
- [30] François, J., Villanueva, M.E. and Hers, H.G. (1988) The control of glycogen metabolism in yeast. I. In vivo interconversion of glycogen synthase and glycogen phosphorylase induced by glucose, a nitrogen source, and uncouplers. *Eur. J. Biochem.* 174, 551–559.
- [31] Vandercammen, A., François, J. and Hers, H.G. (1989) Characterisation of trehalose-6-phosphate synthase and trehalose-6-phosphate phosphatase of *Saccharomyces cerevisiae*. *Eur. J. Biochem.* 182, 613–620.
- [32] Neves, M.J. and François, J. (1992) On the mechanism by which a heat shock induces trehalose accumulation in *Saccharomyces cerevisiae*. *Biochem. J.* 288, 859–864.

- [33] Parrou, J.L. and François, J. (1997) A simplified procedure for a rapid and reliable assay of both glycogen and trehalose in whole yeast cells. *Anal. Biochem.* 248, 186–188.
- [34] Groussac, E., Ortiz, M. and François, J. (2000) Improved protocols for quantitative determination of metabolites from biological samples using high performance ionic-exchange chromatography with conductimetric and pulsed amperometric detection. *Enzyme Microb. Technol.* 26, 715–723.
- [35] Bell, W., Klaassen, P., Ohnacker, M., Boller, T., Herweijer, M., Schoppink, P., Van der Zee, P. and Wiemken, A. (1992) Characterization of the 56-kDa subunit of yeast trehalose-6-phosphate synthase and cloning of its gene reveal its identity with the product of *CIF1*, a regulator of carbon catabolite inactivation. *Eur. J. Biochem.* 209, 951–959.
- [36] Cheng, C., Mu, J., Farkas, I., Huang, D., Goebel, M.G. and Roach, P.J. (1995) Requirement of the self-glucosylating initiator proteins Glg1p and Glg2p for glycogen accumulation in *Saccharomyces cerevisiae*. *Mol. Cell. Biol.* 15, 6632–6640.
- [37] Farkas, I., Hardy, T.A., Goebel, M.G. and Roach, P.J. (1991) Two glycogen synthase isoforms in *Saccharomyces cerevisiae* are coded by distinct genes that are differentially controlled. *J. Biol. Chem.* 266, 15602–15607.
- [38] Strassle, C., Sonnleitner, B. and Fiechter, A. (1989) A predictive model for spontaneous synchronisation of *Saccharomyces cerevisiae* grown in continuous culture. I. *Concept. J. Biotechnol.* 7, 299–318.
- [39] Munch, T., Sonnleitner, B. and Fiechter, A. (1992) The decisive role of the *Saccharomyces cerevisiae* cell cycle behaviour for dynamic growth characterization. *J. Biotechnol.* 22, 329–351.
- [40] Pronk, J.T., Steensma, H.Y. and Van Dijken, J.P. (1996) Pyruvate metabolism in *Saccharomyces cerevisiae*. *Yeast* 12, 1607–1633.
- [41] Larner, J., Takeda, Y. and Hizukuri, S. (1976) The influence of chain size and molecular weight on the kinetic constants for glucose to polysaccharide for rabbit muscle glycogen synthase. *Mol. Cell. Biochem.* 12, 131–136.
- [42] François, J. and Hers, H.G. (1988) The control of glycogen metabolism in yeast. 2. A kinetic study of the two forms of glycogen synthase and of glycogen phosphorylase and an investigation of their interconversion in a cell-free extract. *Eur. J. Biochem.* 174, 561–570.
- [43] Huang, D., Wilson, W.A. and Roach, P.J. (1997) Glucose-6-P control of glycogen synthase phosphorylation in yeast. *J. Biol. Chem.* 272, 22495–22501.
- [44] Pederson, B.A., Wilson, W.A. and Roach, P.J. (2004) Glycogen synthase sensitivity to glucose-6-P is important for controlling glycogen accumulation in *Saccharomyces cerevisiae*. *J. Biol. Chem.* 10.1074/jbc.M312335200.
- [45] Londesborough, J. and Vuorio, O. (1991) Trehalose-6-phosphate synthase/phosphatase complex from bakers' yeast: purification of a proteolytically activated form. *J. Gen. Microbiol.*, 323–330.